What prevented the instantaneous dynamic triggering of the 2019 Mw 7.1 Ridgecrest mainshock by the Mw 5.4 foreshock?

Jeena Yun*, Yuri A. Fialko, and Alice-Agnes Gabriel

Scripps Institution of Oceanography, University of California, San Diego, CA

* Email: j4yun@ucsd.edu

SCEC Contribution #12248, Poster #036

Introduction

The July 2019 M 7.1 Ridgecrest mainshock was preceded by multiple foreshocks including the M 5.4 event. Preliminary models suggest dynamic stress change due to the foreshock of several MPa [1]. In this study, we aim to investigate the physical factors and processes that prevented the instantaneous triggering of the mainshock by the M 5.4 foreshock. We first refine the static and dynamic Coulomb Failure Stress changes (ΔCFS) at the mainshock hypocenter using the 3D dynamic rupture and seismic wave propagation modeling software *SeisSol* [2].

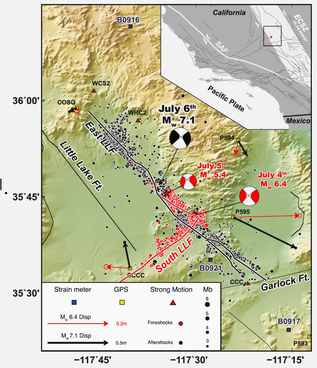

Fig. 1. Locations and focal mechanisms of the mainshock (black) and two largest foreshocks (red) (figure from [3]).

Dynamic & Static ΔCFS

- **Static ΔCFS**
  : A proxy of a permanent change in the applied load after all the waves have passed through

$$\Delta\mathrm{CFS} = \Delta\tau - \mu\Delta\sigma_e$$

τ: shear stress, σ_e: effective normal stress, μ: friction coefficient

- **Peak Dynamic ΔCFS**
  : A proxy of a weakening of the fault zone at the time of the wave passage

$$\max\{\Delta\mathrm{CFS}(t)\} = \max\{\Delta\tau(t) - \mu\Delta\sigma_e(t)\}$$

Workflow

1. Horizontal: put only the foreshock rupture plane into the simulation. Stress tensors on every point on the domain are converted into normal and shear stress on the mainshock fault plane.
2. Vertical: add the mainshock fault plane to the simulation. Normal and shear stress on the mainshock fault plane is directly obtained from the simulation.
3. Repeat steps 1 and 2 for a diverse set of the mainshock nucleation site geometries (depths of 3-7 km; strikes of 320˚-340˚).

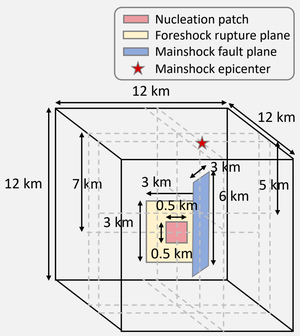

↑ Fig. 2. Dimensions and locations of main features embedded in the model.

↓ Fig. 3. A diagram of workflow

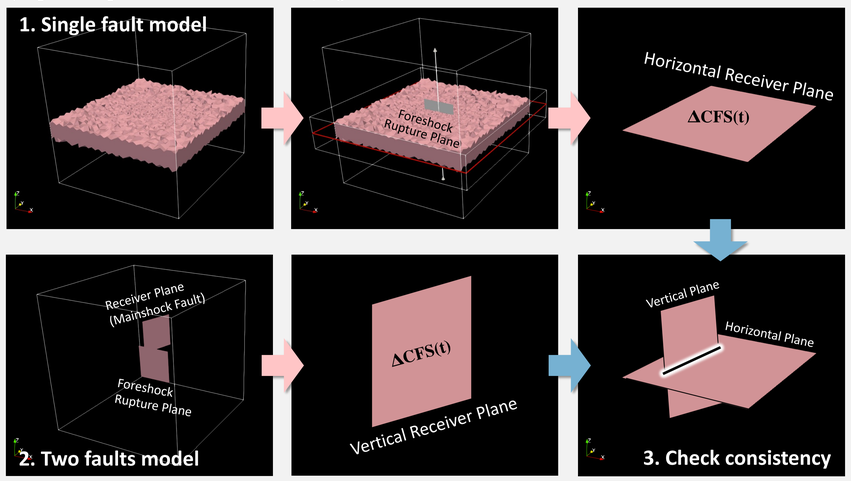

Results – Dynamic and Static Coulomb Stress Changes

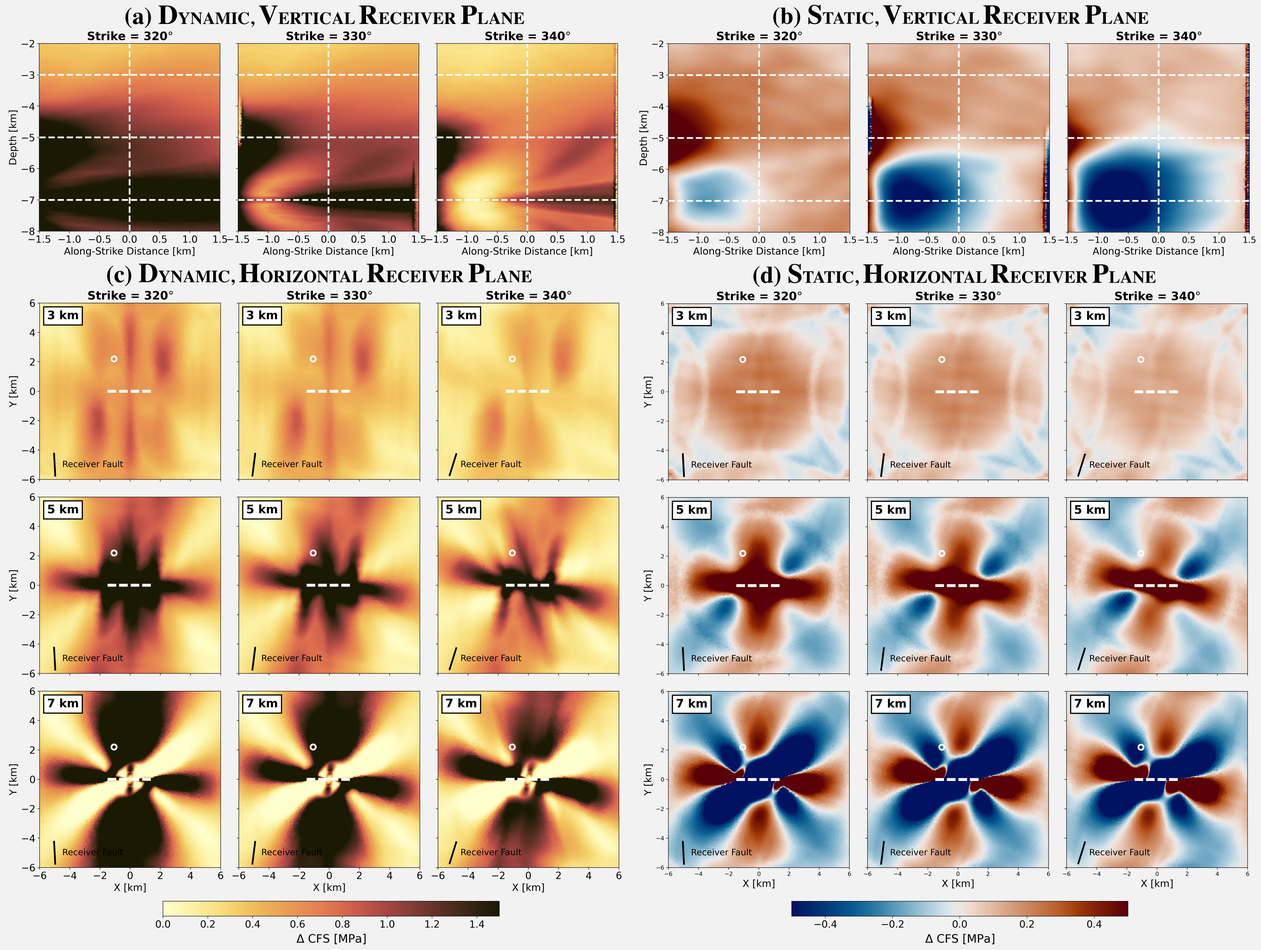

- Peak dynamic ΔCFS are as large as several MPa, while static ΔCFS are mostly of the order of a few hundreds of kPa.
- Peak dynamic ΔCFS decrease with decreasing depth of the hypocenter, and a more northerly strike angle.
- Static ΔCFS are mostly positive at shallower hypocentral depth, while negative values are obtained at greater depth.

← Fig. 4. The ΔCFS values computed from the dynamic rupture modeling. (a-b) Peak dynamic (a) and static (b) ΔCFS on the vertical receiver plane. White dashed lines guide the three depths (3–7 km) used to image the horizontal variation and the along-strike location of the mainshock hypocenter. (c-d) Peak dynamic (c) and static (d) ΔCFS on the horizontal receiver plane. White dashed lines indicate the foreshock rupture plane, and the white circles represent the location of the mainshock hypocenter. Orientation of the assumed mainshock fault plane is shown at the right bottom corner of each panel.

ΔCFS Evolution by Time

- Peak dynamic ΔCFS at the mainshock hypocenter occurs around 1.4 – 1.8 seconds after the nucleation and increases with deeper depth and more westerly strike angle
- Static ΔCFS show stronger negative values with deeper depth and more northerly strikes, consistent with the preliminary estimation[1].
- Stress components resolved on the vertical and horizontal receiver planes are the same as expected.

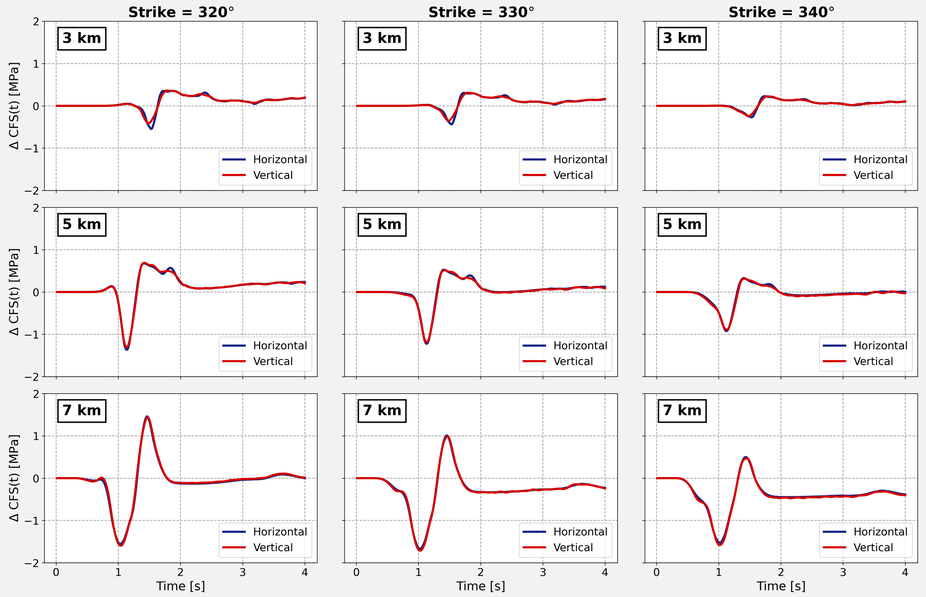

Fig. 5. Evolution of the average ΔCFS as a function of time within a 0.5 km-radius circle centering at the mainshock hypocenter.

Summary & Future Work

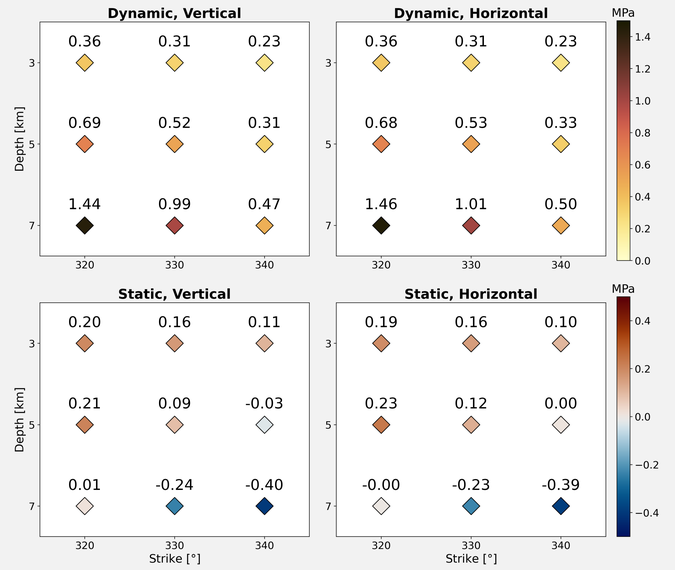

Fig. 6. Predicted dynamic and static ΔCFS as a function of assumed mainshock hypocenter depth and strike angle.

- Peak dynamic ΔCFS at the mainshock hypocenter are as large as several MPa, but decrease with decreasing hypocenter depth and the more northerly strike angle.
- Static ΔCFS at the mainshock hypocenter are of the order of a few hundreds of kPa, and decrease from positive to negative with increasing hypocenter depth, and the more northerly strike angle.
- Our results appear to favor a shallow nucleation depth of the M 7.1 mainshock as suggested by some previous studies[4] because the dynamic stress changes are significantly reduced for the hypocenter depth less than 5 km.
- We plan to use the dynamic stress perturbation predicted by our numerical models in a multicycle rate-and-state framework to test the stability of a future nucleation site under known dynamic loading.

References

[1] Jin, Z., & Fialko, Y. (2020). Finite slip models of the 2019 Ridgecrest earthquake sequence constrained by space geodetic data and aftershock locations. *Bulletin of the Seismological Society of America*, 110(4), 1660-1679.

[2] Krenz, L., Uphoff, C., Ulrich, T., Gabriel, A. A., Abrahams, L. S., Dunham, E. M., & Bader, M. (2021, November). 3D acoustic-elastic coupling with gravity: the dynamics of the 2018 Palu, Sulawesi ear thquake and tsunami. *In Proceedings of the International Conference for High Performance Computing, Networking, Storage and Analysis* (pp. 1-14).

[3] Yue, H., Sun, J., Wang, M., Shen, Z., Li, M., Xue, L., ... & Lay, T. (2021). The 2019 Ridgecrest, California earthquake sequence: Evolution of seismic and aseismic slip on an orthogonal fault system. *Earth and Planetary Science Letters*, 570, 117066.

[4] Lomax, A. (2020). Absolute location of 2019 Ridgecrest seismicity reveals a shallow Mw 7.1 hypocenter, migrating and pulsing Mw 7.1 foreshocks, and duplex Mw 6.4 ruptures. *Bulletin of the Seismological Society of America*, 110(4), 1845-1858.